Mossbauer and AC-susceptibility investigations of the alloy series $FeAl_{1-x}Mn_x$

1991 J. Phys.: Condens. Matter 3 4983

(http://iopscience.iop.org/0953-8984/3/26/018)

J. Phys.: Condens. Matter 3 (1991) 4983–4998. Printed in the UK

Mössbauer and AC-susceptibility investigations of the alloy series $FeAl_{1-x}Mn_x$

M A Kobeissi†
Department of Physics, University of Liverpool, Liverpool L69 3BX, UK

Received 9 October 1990, in final form 11 March 1991

Abstract. Mössbauer and AC-susceptibility measurements have been carried out on the alloy series $FeAl_{1-x}Mn_x$ within the range $0.05 \leqslant x \leqslant 0.40$. Mössbauer spectra reveal the presence of electron charge density and magnetic hyperfine field (B_{hf}) distributions at two iron sites. The charge density rises linearly with Mn concentration while B_{hf} increases non-linearly with x indicating a polarized spin density of the itinerant electrons at the Fe nucleus due to the near neighbouring Fe and Mn magnetic moments. The onset of magnetism is explained by the formation of magnetic moment at the iron atom when Al atoms are removed and by the nearest neighbouring iron clustering. Magnetic measurements indicate the presence of mictomagnetic clusters and show a transition from paramagnetic state to magnetic glass state for all the alloys. No onset of ferromagnetism with increasing x was observed even at the concentration $x = 0.4$, in contrast to that observed in $FeAl_{1-x}Cu_x$ at a lower concentration $x = 0.325$. Comparison of the transition temperatures obtained from Mössbauer and AC-susceptibility measurements indicate relaxations of the magnetic clusters.

1. Introduction

Spin glass magnetism and its phase transition at well defined temperatures and the occurrence of re-entrant ferromagnetic behaviour in binary and ternary alloys with dilute and concentrated transition metals have been the subject of intensive studies in the past few decades [1–6]. A variety of experimental techniques has been used [7–14] and a few theoretical models have been suggested to explain the magnetic interactions occurring in these alloys [15–23]. Whether they are binary alloys, such as $Fe_{1-x}Al_x$, $Au_{1-x}F_x$ and $Fe_{1-x}Cr_x$, or ternary ones such as $FeAl_{1-x}T_x$ and $Fe_{1-x}T_xSi$ (T being a 3d transition metal) occupational disorder and site selectivity of the atoms in the crystals occur leading to the appearance of certain interesting magnetic behaviours [1–3]. It is believed that competing interactions among the ferro- and antiferromagnetic moments take place [2, 3, 5–8, 19]. In addition, these systems do not necessarily possess a conventional order parameter as is the case in pure ferro- and antiferromagnets, and many anomalous phenomena have been observed with the variations of the temperature of the alloys or the concentration of the transition metal [11, 14]. A systematic and comprehensive theory on the origin, nature and mechanism of the magnetic interaction in these classes of alloys is still lacking and one has to rely presently on a more phenomenological approach through detailed experimental results based on both microscopic

† Present address: Department of Physics, UAE University, PO Box 17551, United Arab Emirates.

0953-8984/91/264983 + 16 $03.50

and macroscopic measurements in order to clarify any ambiguity which might accompany either method.

One interesting set of alloys whose study can help us understand some aspects of magnetic interactions is the alloy series $FeAl_{1-x}T_x$ whose parent alloy FeAl has been studied extensively by several authors [15, 24–26]. The structural and magnetic properties of the alloy series $FeAl_{1-x}T_x$ (T = Ti, V, Mn, Cr, Cu) have been investigated recently by Okpalugo *et al* [27, 28] and Saleh *et al* [29] who employed x-ray diffraction, magnetization and neutron diffraction techniques. They have determined site occupation and the onset of magnetism in the above-mentioned alloys as the concentration x of the transition metal T was increased. They have observed the appearance of spin glass, mictomagnetism and superparamagnetic behaviour, but no affirmative explanation of these effects has been given. In a recent work on $FeAl_{1-x}Cu_x$ [30] and $FeAl_{1-x}Cr_x$ [31] using Mössbauer and low-field AC-susceptibility measurements we have established that these alloys exhibit spin glass characteristics and re-entrant ferromagnetism. They became ferromagnets as x was increased and a magnetic phase diagram as a function of x was given, thus clarifying their magnetic behaviour observed in the bulk measurements [27, 29].

The study of the parent alloy $Fe_{1-x}Al_x$ has shown spin glass, re-entrant ferromagnetism, superparamagnetism and parasitic antiferromagnetic spin alignment as x is varied [11], but the equiatomic alloy FeAl is non-magnetic, even at 4.2 K and it crystallizes on slow cooling into the B2 structure of inter-penetrating cubic Fe and Al lattice [24–26] where the site ordering is complete.

For the alloy $FeAl_{1-x}Mn_x$ neutron diffraction showed that the system FeAl transforms into $B2_3$ upon Mn substitution for Al and at $x = 0.40$ the Mn atoms enter the Al site and the Fe site in the ratio 3:2 [28]. Magnetically, this alloy series turned out to be more complex than $FeAl_{1-x}Cu_x$, as is evidenced in the magnetization measurements by Okpalugo *et al* [28]. Since Mn is antiferromagnetic, and its atoms might possess magnetic moment when substituted in $FeAl_{1-x}Mn_x$, there is no firm evidence from these authors' data whether the system has ferromagnetic or antiferromagnetic properties when x is varied and spin glass properties were not well confirmed. Their measurements on the spontaneous magnetization for a given x as a function of temperature showed no trend of normal behaviour and no T_c could be found even for the highest concentration ($x = 0.40$) studied.

To complete the picture of a systematic study on the alloy series $FeAl_{1-x}T_x$ and in order to obtain a better understanding of their magnetic properties, we present in this report low-field AC-susceptibility measurements and Mössbauer spectroscopy results on the system $FeAl_{1-x}Mn_x$ ($0.05 \leqslant x \leqslant 0.40$) and it is our aim to study the microscopic environments of localized magnetic moments, the electronic transfer, site occupation, and structural properties of this system. We will attempt to clarify the ambiguous behaviour which is apparent in the magnetization measurements [28].

2. Experimental technique

The alloys we have used in this experiment are in powder form and were those used by Okpalugo *et al* [28]. Their fabrication and heat treatment are reported in their publication [27].

2.1. Mössbauer measurements

The alloys were used as Mössbauer absorbers which were made by spreading the powder finely and homogeneously on a circular masking tape. This was enclosed in a polypropylene sample holder. The Mössbauer source of 50 mCi diffused in a Rh matrix was mounted on a standard constant acceleration drive with double ramp. The Mössbauer spectrometers were calibrated with a thin α-Fe foil at room temperature and the isomer shift values are quoted relative to this calibration. The folded Mössbauer spectra showed a flat background.

The Mössbauer transition temperatures T_{hf}, indicated by the collapse of the hyperfine field, were determined by the linewidth narrowing when the alloy goes from the magnetic state to the paramagnetic state as the temperature T is increased. Just above T_{hf} the linewidth remained constant, an indication of the disappearance of the hyperfine field. For the T_{hf} measurements we have used a He flow cryostat with a variable temperature which was accurate to ± 0.5 K. The magnetic spectra recorded for the investigation of the hyperfine field distributions $P(B_{hf})$ as a function of the Mn concentration x were obtained at 4.2 K in a He cryostat.

These spectra were analyzed in terms of a probability distribution $P(B_{hf})$ of the hyperfine field B_{hf} using a least squares fitting program [32]. Smoothing and boundary conditions were applied to the subspectral area minimization procedure, based on the technique proposed by Le Caer *et al* [33]. Quadrupole splitting, as will be shown below, was found to be negligible and linear correlation between increasing isomer shift and decreasing hyperfine field was assumed. The justification of this assumption will be discussed in sections 3.1.1 and 4.2.

2.2. Low-field magnetic AC-susceptibility measurements

For the AC-susceptibility (χ_{AC}) measurements the samples were prepared by compressing each alloy into a nylon holder to form a cylinder of 1.5 mm diameter and 30 mm length. Each sample was held parallel to the axis and at the centre of a pick-up coil of a balanced mutual inductance bridge. This was operated at a frequency of 15 Hz with an RMS field of 8 μT. A static field of 12 mT was applied parallel to the AC-field and to the long axis of the sample. The temperature control system of the He flow cryostat stabilized the temperature to better than 0.5 K in the range 4.2–200 K. The values of χ_{AC} versus temperature were recorded over a complete down and up temperature cycle starting with the highest temperature. The transition temperature T_f indicating the freezing of the spin glass was marked as the maximum of the cusp of the χ_{AC} graphs. No ordering temperature T_c was observed in these alloys within the concentration range of $0.05 \leqslant x \leqslant 0.40$ studied in this report.

3. Results

3.1. Mössbauer results

3.1.1. The variation of isomer shift with x. The room temperature spectra are shown in Figure 1 for all the samples studied. They exhibit a broadened asymmetric single line which, when fitted to a singlet, gives an average full width at half maximum increasing from 0.4 mm s^{-1} for $x = 0.05$ and 0.10 to 0.48 mm s^{-1} for the rest of the concentrations up to $x = 0.40$. The asymmetric profile of these lines is an indication of the distribution in

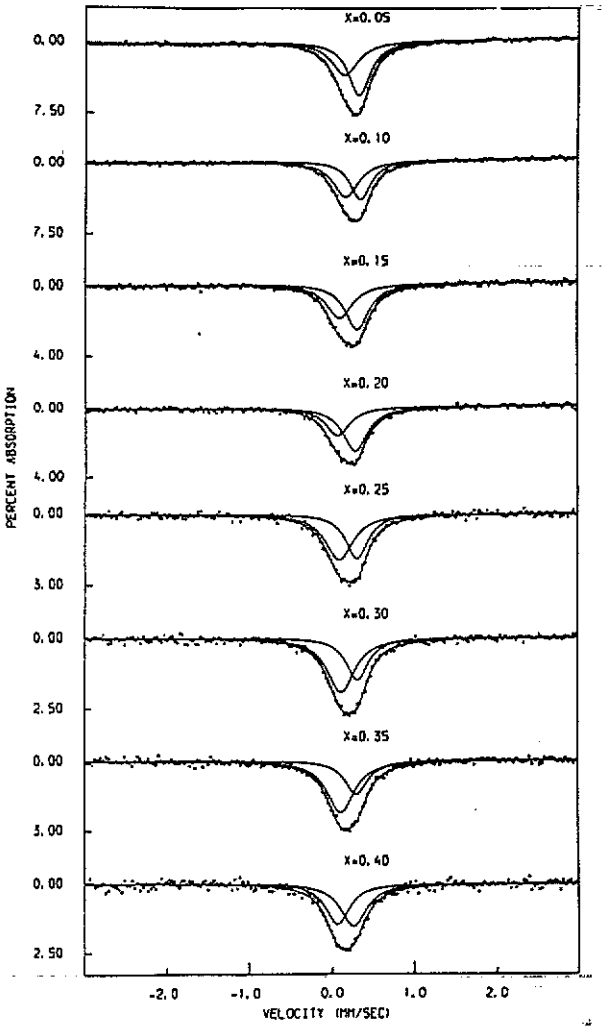

Figure 1. Mössbauer spectra taken at room temperature for various concentrations x of Mn. Isomer shifts are quoted relative to metallic α-iron. Notice the asymmetric lineshape, which consists of two singlets, with which the spectra were best fitted.

the electron density at the Fe sites surrounded by different combinations of neighbouring atoms. Moreover, each of these lines was best fitted with two singlets reflecting the existence of two Fe sites each with a different distribution of atomic surrounding and thus different isomer shifts δ_1 and δ_2. Fitting the spectra with two singlets was based on their shape and profile and on the fact that the χ-squared values in all fits were closer to unity than those obtained from one singlet fits (for example, for $x = 0.30$, fits gave $\chi = 0.999$ for two singlets while $\chi = 1.11$ for one singlet). The mean isomer shift value δ is obtained from the weighted velocity positions of the two singlets by their corresponding areas. The values for the isomer shift δ thus obtained and those of δ_1 and δ_2 are listed in table 1. The variation of δ with x is shown in figure 2. Unlike the δ values obtained previously [34] for $FeAl_{1-x}Cu_x$, these values show a heavy scatter from a straight line,

Table 1. *The first column shows the Mn or the Cu concentration x in the alloy series $FeAl_{1-x}Mn_x$ and $FeAl_{1-x}Cu_x$. The second and third columns list the isomer shift of each singlet in figure 1. The fourth column lists the average isomer shift values at various Mn concentrations, while the fifth column indicates the isomer shift in $FeAl_{1-x}Cu_x$ taken from reference [34] for comparison. The isomer shifts were taken at 300 K for both series and are quoted relative to α-iron metal. The error in δ is estimated to be ± 0.07 mm s^{-1}. The mean hyperfine field values $\overline{B_{hf}}(0)$ at 4.2 K for each series are listed in columns 6 and 7 ($\overline{B_{hf}}(0)$ values for $FeAl_{1-x}Cu_x$ were taken from reference [34]). The hyperfine transition temperatures T_{hf} and the freezing temperatures T_f for some alloys in the series $FeAl_{1-x}Mn_x$ are listed in columns 8 and 9 respectively. The non-linear rise of $\overline{B_{hf}}(0)$ in $FeAl_{1-x}Mn_x$ is noticeable as compared to that in $FeAl_{1-x}Cu_x$.*

	The two sites Isomer shift in $FeAl_{1-x}Mn_x$		*Mean isomer shift*		Mean hyperfine field $\overline{B_{hf}(0)}$ [KG]		Transition temperature in $FeAl_{1-x}Mn_x$	
Mn or Cu content x	δ_1 (mm s^{-1})	δ_2 (mm s^{-1})	$FeAl_{1-x}Mn_x$ δ(mm s^{-1})	$FeAl_{1-x}Cu_x$ δ(mm s^{-1})	$FeAl_{1-x}Mn_x$ $\overline{B_{hf}(0)}$	$FeAl_{1-x}Cu_x$ $\overline{B_{hf}(0)}$	Hyperfine T_{hf} (K)	Freezing T_f (K)
0.05	0.14	0.32	0.24	0.26	24.5 ± 2	31		
0.100	0.16	0.34	0.24	0.24	34.1 ± 2	59		
0.150	0.10	0.31	0.21	0.22	52.0 ± 2	81		
0.200	0.07	0.28	0.20		59.4 ± 2			5 ± 2
0.225				0.21				
0.250	0.08	0.30	0.18	0.19	65.1 ± 3	126	20 ± 3	
0.300	0.11	0.31	0.18		68.2 ± 3		23 ± 2	32 ± 3
0.325				0.18		166		
0.350	0.10	0.29	0.16		84 ± 3			
0.400	0.06	0.26	0.16		85 ± 3	203	45 ± 3	30 ± 3

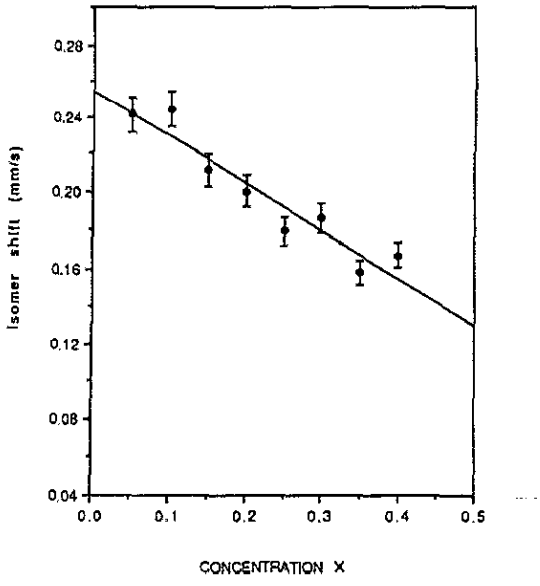

Figure 2. Graph of the weighted isomer shift δ versus Mn concentration x. The values of δ are obtained from the weighted two singlets positions with the total area of the spectrum.

similar to that obtained by Omari *et al* [35], but the general trend is the same in both alloys, a decrease of δ with increasing x, and is attributable to the same origin whereby with increasing x the population of the 3d electrons around the Fe atom decreases and therefore reduces the shielding of the s shell electrons and increases their charge density at the Fe nucleus. For Fe^{57} this means a decrease in the isomer shift.

3.1.2. Saturation hyperfine field $B_{hf}(0)$ at 4.2 K and its distribution with x. The Mössbauer spectra recorded at 4.2 K for all the alloys are shown in figure 3. The broad features of the spectra, indicating the spread of different local environments around the Fe nuclei, were fitted to a distribution of hyperfine fields $P(B_{hf})$ with isomer shift and quadrupole splitting left as free parameters. Their histograms, derived from fits of the spectra of figure 3, are shown in figure 4. Our choice of fitting the spectra to a hyperfine field distribution is based on our low field AC-susceptibility measurements, whereby a freezing of the magnetic moments at 4.2 K has been observed for most of the samples so that magnetic fluctuations at this temperature are less dominant and the relaxation time distribution method was therefore not applied. It can be seen that $P(B_{hf})$ consists of two broad maxima, representing a low-field and a high-field average value, $\overline{B_{LF}}(0)$ and $\overline{B_{HF}}(0)$, respectively, which is similar to that found by Brand *et al* [36] in AuFe. The presence of these two distinct maxima reflects the existence of two Fe sites each with different local environments, which is consistent with the profiles of the spectra and the isomer shift values at room temperature. In addition we notice in figure 4 that the width of the low-field distribution increases with Mn concentration x while that of the high field remain almost constant. It is worthwhile mentioning that the two site characteristic, as mentioned above, has been realized in the isomer shift measurements in figure 1 which we took prior to $B_{hf}(0)$ measurements at 4.2 K (see below).

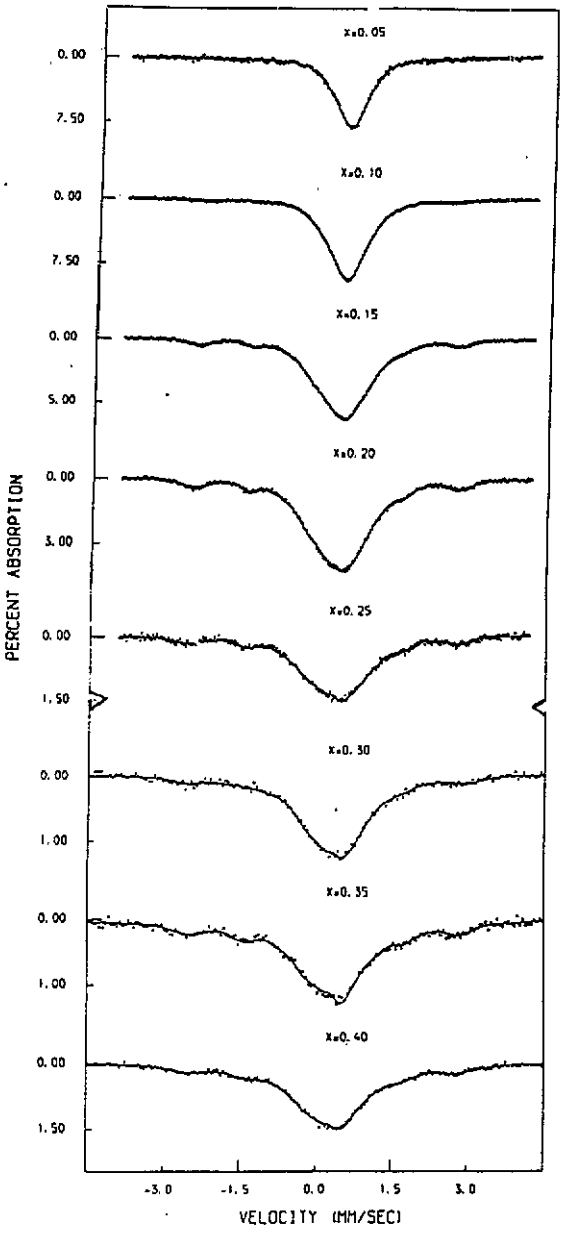

Figure 3. Mössbauer spectra for the complete set of $FeAl_{1-x}Mn_x$ alloys taken at 4.2 K. The spectra are fitted with a distribution of hyperfine fields with the isomer shift and quadrupole splittings left as free parameters.

The overall mean value $\overline{B_{hf}(0)}$ of the hyperfine field for each concentration x is evaluated from each histogram and is listed in table 1. The $\overline{B_{hf}(0)}$ value increases slowly and non-linearly with x. The correlation between increased hyperfine field (thus the onset of magnetism) and decreased isomer shift incorporated in the fits is implicit in the model whereby decreasing the 3d electrons population of the Fe atom causes an increased

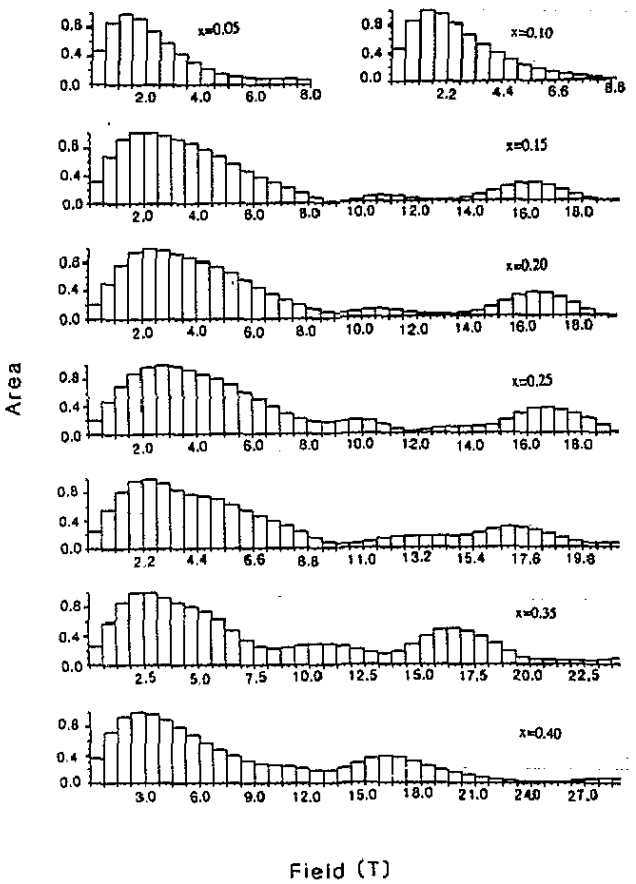

Figure 4. The distribution of hyperfine fields obtained from fitting the spectra of figure 3. Notice the distinct two maxima corresponding to low-field $\overline{B_{LF}}(0)$ and high-field $\overline{B_{HF}}(0)$ distributions and the almost constant position of $\overline{B_{HF}}(0)$. The area is normalized. Notice that the horizontal scale of the field axis is different for each histogram.

s-electron density at the nucleus. In such a system increased $B_{hf}(0)$ and decreased δ are correlated provided that the iron 3d population increases the mean spin value $\langle S \rangle$ of the atom by removing electrons with spins antiparallel to the majority direction.

3.1.3. Measurements of the Mössbauer ordering temperature T_{hf}. The transition temperature T_{hf} at which the hyperfine field collapses, and above which the alloys are paramagnetic, was determined from the graphs of the variations with temperature of the average linewidth of the spectra in the vicinity of T_{hf} as can be seen in figure 5. To obtain the average linewidth, the spectra were fitted to a singlet, instead of two singlets, just below and above the T_{hf}. This method is sensitive enough to determine T_{hf}. Above T_{hf} the average linewidth remains constant while below T_{hf} it increases rapidly as is shown for typical spectra in figure 6. The line broadening denotes the appearance of magnetic hyperfine interaction at the iron nuclei which varies slowly compared to the Mössbauer measuring time of 10^{-7} s. Above T_{hf} the B_{hf} fluctuations are much faster and

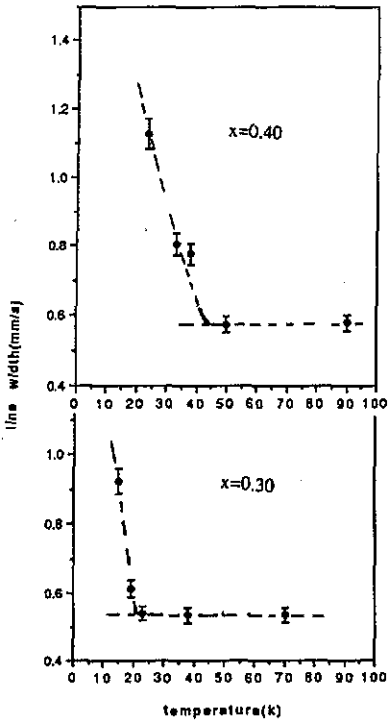

Figure 5. The average linewidth variation of the spectra just below and above the Mössbauer transition temperature T_{hf}. The average linewidth remains constant in the paramagnetic state and increases rapidly when the temperature crosses into the magnetic state. The graphs were used to determine T_{hf}.

the average linewidth therefore remains constant. Typical values of T_{hf} for some alloys are shown in table 1.

3.2. AC-susceptibility (χ_{AC}) results

The range of the alloy series $FeAl_{1-x}Mn_x$ comprises values of Mn concentration x = 0.05, 0.10, 0.15, 0.20, 0.25, 0.30, 0.35 and 0.40, but only values of $x > 0.20$ with a response of χ_{AC} and a measurable maxima could be obtained within the temperature range of our measuring instruments. Graphs of the variations of χ_{AC} with temperature are shown in figure 7 for $x = 0.30$ and 0.40. For $x = 0.20$ the graph showed a sharp cusp shape but its maximum was just at the lowest available measuring temperature of ≈ 5 K. The maximum of the χ_{AC} graph corresponds to the transition temperature T_f at which the fluctuations of the Fe magnetic moments in the paramagnetic state begin to freeze into different static orientations, thus forming spin glass clusters as the temperature is lowered. It is seen from table 1 that T_f increases slowly with increasing Mn concentration x. For the sample $x = 0.40$, the highest value available to us, the cusp is rounded, while for $x = 0.30$ the χ_{AC} response is higher above T_f and consists of a long slowly decaying tail for a wide range of temperature. This is similar to the behaviour of the χ_{AC} measurements in the alloy $Fe_{68}Al_{32}$ observed by Shull *et al* [11].

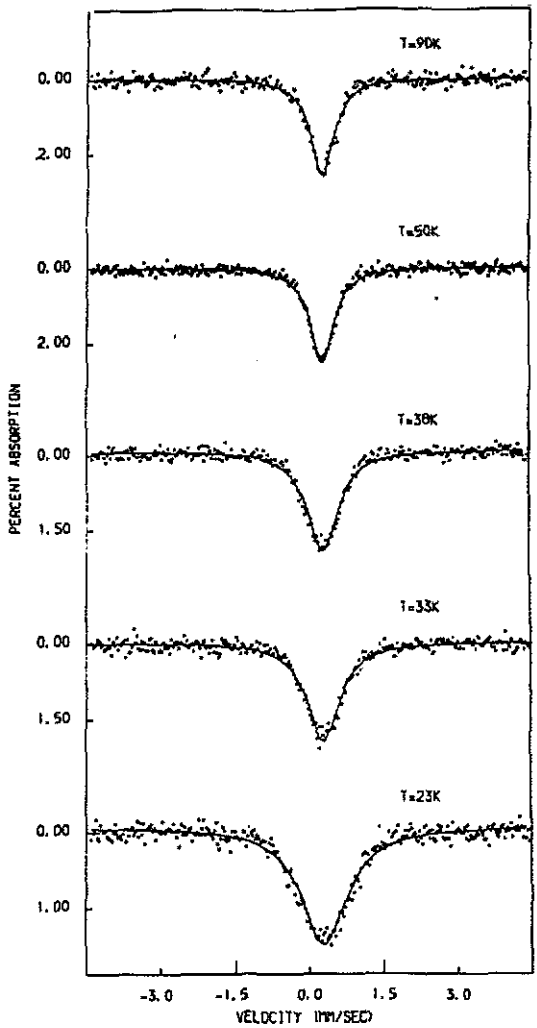

Figure 6. Mössbauer spectra for $x = 0.40$ showing the change in the linewidths at various temperatures. Such spectra for each concentration x were fitted to a single lineshape in order to extract the average linewidths which were used to construct the graphs in figure 5 for the determination of T_{hf}. Notice that the spectra do fit better to the single lineshape above T_{hf} than they fit below T_{hf} due to line broadening.

The effect of static applied field of $B_{ext} = 12$ mT on χ_{AC} versus temperature for a sample of $x = 0.40$ is shown also in figure 7. The field was applied starting at the higher end of the sample temperature. It can be seen that the field compresses the maximum of the cusp which is a typical behaviour of spin glass systems for a transition from paramagnetic to spin glass phase [2, 3]. The field influence has shifted the cusp maximum about 8 K toward a lower temperature, which did not occur in our previous studies [30, 31] of $FeAl_{1-x}Cu_x$ and $FeAl_{1-x}Cr_x$, and it is an effect which we will attempt to explain in a later section.

4. Discussion

As we have mentioned above, the parent alloy of the series $FeAl_{1-x}Mn_x$ used in this

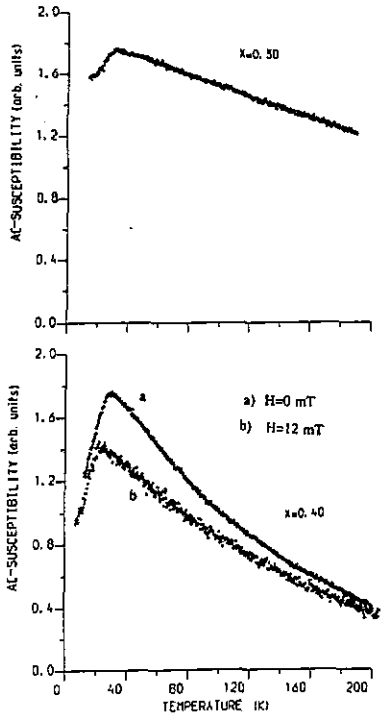

Figure 7. Graphs of the AC-susceptibility χ_{AC} versus temperature for alloys with $x = 0.40$ (bottom) and $x = 0.30$ (top). The effect of an applied field of 12 mT on χ_{AC} for $x = 0.40$ is noticeable in the suppression of the graph and in the shift of the maximum toward lower temperature of about 8 K. A slight rounding of the cusp in the applied field is observed. The values of T_f are obtained from the position of cusps in zero field. Notice the difference in the dependence of χ_{AC} on the temperature in both alloys ($x = 0.40$ and 0.30) above T_f. χ_{AC} is in arbitrary units of the same scale for both alloys.

experiment is the equiatomic alloy FeAl which crystallizes into the ordered B2(CsCl) structure [24–26]. For the series $FeAl_{1-x}Fe_x$ the magnetic Fe atom corresponding to $x > 0$ can be regarded as displacing an Al atom of the B2 structure and therefore such an Fe atom has eight Fe nearest neighbours bearing magnetic moments. In this case the nearest neighbours clusters build up most quickly and a magnetic state occurs as x increases [15]. For the series $FeAl_{1-x}Cu_x$, it has been shown [30] that the non-magnetic Cu atoms substitute randomly on the Fe and Al sublattices of the ordered $Fe_{0.5}Al_{0.5}$. The substitution of Cu on the Al site creates no Fe nearest neighbour clusters but substitution on the Fe site displaces the Fe atoms into the Al site forming nearest neighbours and thus promoting Fe atom clustering. This mechanism implies that Cu substitution should be approximately half as effective in promoting Fe atom clusters as the Fe one. In a recent Mössbauer study [30, 34] we have shown the sharp rise of the Mössbauer transition temperature T_{hf} as well as the hyperfine field $B_{hf}(0)$ upon increasing Cu concentration in this series, indicating the rapid build-up of Fe clusters which has promoted the formation of spin glass, re-entrant ferromagnetism and finally a ferromagnetic state as x increases. The alloy series $FeAl_{1-x}Mn_x$ behaves structurally similarly to $FeAl_{1-x}Cu_x$ but magnetically it is more complex as has been shown by Okpalugo *et al* [28]. The Mn, unlike Cu, is an antiferromagnet (whether α-Mn or γ-Mn) and its atom might still bear

a magnetic moment when substituted into this alloy, whose structure remains $B2_3$ [28] upon substitution up to $x = 0.40$, where Mn enters the Al site preferentially in the ratio 3:2. These structural and magnetic complexities will be discussed in the following sections.

4.1. The variation of the isomer shift δ with x

The Mössbauer spectra give information on the microscopic environments surrounding the Fe atoms; thus localized changes on the atomic levels can be detected. The spectra shown in figure 1 each exhibit double singlets with isomer shifts δ_1 and δ_2 which are different in values but their trend in decreasing with increasing x is the same as the average value δ shown in figure 2. The presence of double singlets in the spectra reveals the existence of two clustered regions. The low value isomer shift δ_1 corresponds to a surrounding of an Fe atom with heavier Fe clustering while the higher δ_2 corresponds to a surrounding of an Fe atom formed by a combination of Fe, Mn and Al atoms. It is seen in figure 1 that the intensity of the lower energy peak increases as the Mn concentration is increased, displacing more Fe atoms into a configuration rich in Fe nearest neighbours. At the concentration $x = 0.40$ where the Mn preferentially substitutes onto the Al sites the intensity of this component decreases. This decrease in isomer shift with increasing Mn concentration x or decreasing electron density in the conduction band, can be accounted for by the change in the occupation of the Fe 3d shell. This 3d shell, lying energetically within the conduction band, contains bound and virtually bound electrons. These 3d electrons act to screen the Fe nucleus from the atomic 3s and 4s electrons which contribute to the s electrons' charge density at the nucleus. Thus when Al is replaced by Mn, whose electron donation to the conduction band is less than that of Al, the 3d electron density falls and the s electrons at the Fe nucleus rise thus producing the decrease of the overall isomer shifts observed in figure 2. A similar effect of the increased isomer shift, or decrease in charge density at the Fe nucleus, with increasing Al content in the FeAl alloy was observed by Johnson *et al* [24] and Stearns [25]. It should also be noticed that the equivalency of the average δ values in this work with those obtained (see table 1) in the series $FeAl_{1-x}Cu_x$ indicates that the s-electron charge density at the Fe nucleus in both series are nearly the same. These results may be understood in terms of the shared trapping of the two valence s electrons of Mn by the d shell of the Mn and that of Fe atoms. Trapping of electrons by the Mn d shell may also weaken its magnetic moment provided it possesses one.

4.2. The variations of the saturated hyperfine field $B_{hf}(0)$ and the ordering temperature T_{hf} with x

The fitted Mössbauer spectra recorded at 4.2 K, and shown in figure 3, and the hyperfine field distribution extracted from these spectra, and shown in figure 4, show the following characteristics.

(*a*) A broad distribution of hyperfine field is necessary to fit the spectra of all alloys with $x \geqslant 0.05$.

(*b*) The mean value of the saturated hyperfine field $B_{hf}(0)$ increases as x increases but slowly and non-linearly.

(*c*) The distribution appears to consist of two broad maxima of low-field values of $B_{LF}(0) \approx 3$ T and high-field value of $B_{HF}(0) \approx 17$ T. The value of B_{LF} increases slightly

more rapidly than that of B_{HF} which remains almost constant as x increases. Their area ratio is close to 3:2 in favour of the low field for $0.25 \leqslant x \leqslant 0.40$ and 2:1 for $0.15 \leqslant x \leqslant 0.20$.

The hyperfine field distributions shown in figure 4 are due to the range of near neighbouring environments. The isomer shift results showed that the number of 3d electrons decreases as x increases. This situation generates the formation of a local 3d moment at the Fe atom, provided that the number of 3d electrons on the Fe exceeds 5, at which value the 3d shell is half filled with electrons of parallel spin, thus giving maximum value of the mean spin density $\langle S \rangle$ at the iron atom. Following the concept that the contact mechanism is the main contributor to the hyperfine field $B_{hf}(0)$, this latter must be proportional to $\langle S \rangle$ which is determined by the mean number of bound and virtually bound electrons in the Fe 3d shell. But for the Al rich alloys the mean number of Fe 3d electrons is greatest, and since the number of electrons in excess of five have opposite spin to the majority direction, the value of $\langle S \rangle$ is reduced. With the removal of Al with increasing x, the spin minority sense electrons are decreased and the $\langle S \rangle$ and $B_{hf}(0)$ increase. The mean spin $\langle S \rangle$ at the Fe atom could be influenced drastically by near neighbour atoms, especially those carrying parallel or anti-parallel magnetic moments. In this work we found that the hyperfine field $B_{hf}(0)$ in $FeAl_{1-x}Mn_x$ is much lower than $B_{hf}(0)$ obtained in the alloy series $FeAl_{1-x}Cu_x$ (see table 1) for a given concentration x. This indicates that the presence of Mn as a near neighbour of the Fe atom reduces the spin density value at the Fe atom and thus the hyperfine field B_{hf}. Such effects have been observed by several researchers [10, 12, 13] in the alloy series $Fe_{3-x}Mn_xSi$, which is structurally similar to ours, using spin-echo NMR, Mössbauer effect and neutron diffraction.

Although the isomer shifts in $FeAl_{1-x}Mn_x$ and in $FeAl_{1-x}Cu_x$ alloys are found to be equivalent and thus the generated localized magnetic moment in the d shell of the Fe atom should be the same, this is not to be true for their $B_{hf}(0)$ values, since the increase of the s electron's charge density at the Fe nucleus does not necessitate the increase of the s electron's spin density at that nucleus, for the spin density depends on both signs of the spin. Thus the hyperfine field at the Fe nucleus can be seen as the result of the contribution of the core s electron polarization due to the localized d moment of the Fe itself as well as the polarization of the s-conduction electrons at the near neighbour Fe and Mn atoms. Such $B_{hf}(0)$ is therefore not necessarily linearly proportional to the Mn concentration x of the same magnitude as it is in $FeAl_{1-x}Cu_x$, since Mn atoms and their polarizing effects seem to have a reducing consequence on the B_{hf} values in $FeAl_{1-x}Mn_x$ while such an effect is absent in $FeAl_{1-x}Cu_x$.

When the $B_{hf}(0)$ distribution was fitted to Mössbauer spectra at 4.2 K, the obtained correlation constant a [30] between B_{hf} and δ was almost the same for all concentration values of x and ranged between $a = -15$ and -19, thus giving additional confidence in our analysis. The isomer shift value δ obtained from these spectra decreased from 0.42 mm s^{-1} for $x = 0.05$ to 0.37 mm s^{-1} for $x = 0.40$ as x increased which is consistent with the δ trend in the room temperature measurements. The quadrupole splitting Δ for all concentrations x was close to 0.05 mm s^{-1} (except for $x = 0.05$ where $\Delta =$ 0.01 mm s^{-1}) which is relatively small, and reveals the close cubic symmetry of the system. The double peak in the B_{hf} distribution, which is similar to that obtained for the $FeAl_{1-x}Cu_x$ alloy [30] but more distinct in the present case, is in line with the isomer shift distribution present in the double singlets of the spectra at room temperature, with the low isomer shift δ_1 corresponding to $\overline{B_{HF}}(0)$ and the high δ_2 corresponding to

$\overline{B_{LF}}(0)$, since an Fe atom surrounded by mainly Fe atoms environments possesses higher hyperfine field value, while an Fe atom surrounded by a composition of Fe, Mn and Al atoms will possess a lower field value. Thus in the alloys $FeAl_{1-x}Mn_x$ we have two cluster sites representing two coexisting magnetic states in agreement with theoretical prediction [16, 20] and with similar results obtained in binary alloys such as AuFe [36]. These two states cannot be attributed to two structural phases, since these alloys remain single phase with the variation of x as was shown in the neutron diffraction and x-ray measurements [28].

The area ratio of the low-field and high-field distributions is close to 2:1 for $0.15 \leqslant x \leqslant 0.20$ and 3:2 for $0.25 \leqslant x \leqslant 0.40$ in favour of the low field. The latter value is in agreement with the neutron diffraction results [28] in that Mn enters the Al site and Fe site with the ratio 3:2 respectively. This result agrees also qualitatively with the isomer shift findings discussed above. The almost constant value of $\overline{B_{HF}}(0)$ indicates that the Fe magnetic moment at the Al site remains constant with increasing x, while the Fe magnetic moment at the Fe site does not rise rapidly, as is the case in the $FeAl_{1-x}Cu_x$, but increases slowly due to the presence of the Mn as a reducing environment to the Fe magnetic moment. The constancy of $\overline{B_{HF}}(0)$ agrees with the results of the similar alloy series $Fe_{3-x}Mn_xSi$ [10–13].

The measurements of the Mössbauer transition temperatures shown in figure 5 and table 1 for some values of x indicate a slow and non-linear increase of T_{hf} as x increases, in contrast to the alloy series $FeAl_{1-x}Cu_x$, where T_{hf} increased more rapidly with increasing x [30]. The increase of T_{hf} conforms with the increase of $B_{hf}(0)$ in both alloys, but the magnetic coupling in $FeAl_{1-x}Mn_x$ is weaker than that in $FeAl_{1-x}Cu_x$.

4.3. The AC susceptibility (χ_{AC}) values

In figure 7 we present the characteristics of χ_{AC} for $x = 0.30$ and $x = 0.40$ as a function of temperature. The figure shows also the effect of applied magnetic field H on χ_{AC} for $x = 0.40$. The measurements of χ_{AC} for $x = 0.20$ showed a sharp cusp, similar to those reported for the $FeAl_{1-x}Cu_x$ series [30] which is typical of spin glass behaviour [2, 5, 6]. Its maximum lay just at the limit of our temperature measuring instruments of $T_{hf} \approx 5$ K. The graphs of χ_{AC} versus T show that in the series $FeAl_{1-x}Mn_x$ for $\leqslant 0.40$ there is no evidence for a transition to a ferromagnetic phase such as seen in the series $FeAl_{1-x}Cu_x$ with $x \geqslant 0.3$ and in $FeAl_{1-x}Cr_x$ with $x \geqslant 0.35$.

The variation of χ_{AC} with decreasing temperature for $FeAl_{1-x}Mn_x$ alloys with $x \geqslant 0.20$ shows a transition from a paramagnetic phase to a spin glass phase similar to those observed in the series $FeAl_{1-x}Cu_x$ and $FeAl_{1-x}Cr_x$. The change in the χ_{AC} versus T graph when a field of 12 mT is applied is also similar to that observed in the $FeAl_{1-x}Cu_x$ and $FeAl_{1-x}Cr_x$ systems. However, the detailed form of the graph for the $FeAl_{0.7}Mn_{0.3}$ sample shows behaviour that is difficult to reconcile with the other results. In this sample for temperature greater than that of the observed cusp, the decrease of χ_{AC} with increasing temperature is much slower than for other samples. It is unexpected that the temperature of the cusp T_f is higher for this $x = 0.30$ sample than for $x = 0.40$ sample and, interpreting the cusp as spin glass freezing temperature occurring at T_f, it is difficult to understand why for this sample $T_f > T_{hf}$ the temperature at which a magnetic hyperfine field is observed. Susceptibility behaviour similar to that observed for this $x = 0.30$ sample has been reported by Shull *et al* [11] for alloys near the composition $Fe_{68}Al_{32}$.

Finally, a few statements can be made on the magnetic fluctuation observed in this work, although this is beyond the scope of this paper. Comparing T_f and T_{hf} listed in

table 1, one can see that for $x = 0.40$, T_{hf} is much higher than T_f. This is most probably due to fluctuations of the magnetic moments, where Mössbauer short detection time of $\approx 10^{-7}$ s can see slow fluctuations as an average static hyperfine field. This is typical of many spin glass alloys [3, 12, 30, 31] but it is not a general rule as is seen in our case for $x = 0.30$ where $T_f > T_{hf}$. Such differences in T_f and T_{hf} might occur and are due probably to annealing or sample preparation problems, where phase segregation might take place and iron moments in this case do not take part in the 'freezing' at exactly the temperature T_f, but rather at a lower one. Mössbauer spectra recorded in the vicinity of T_{hf}, as shown for typical spectra in figure 6, and which were used mainly to determine T_{hf}, showed no superparamagnetic behaviour for $x = 0.30$ or $x = 0.40$, but in order to confirm such behaviour, more statistics in the spectra and more refined steps on the temperature scale must be taken.

5. Conclusion

Contrary to what we found in $FeAl_{1-x}Cu_x$ [30] and $FeAl_{1-x}Cr_x$ [31], in this investigation, we found no evidence of the appearance of ferromagnetism or re-entrant ferromagnetic properties in the $FeAl_{1-x}Mn_x$ series within the range $0.05 \leqslant x \leqslant 0.40$, but spin glass characteristics remain the dominant properties in these alloys. It seems that anti-ferromagnetic moments break the long range interactions in the systems and spin glass regions are formed. Higher concentrations of Mn are needed to establish whether a crossover from cluster glass state to ferromagnetism is possible in this system as we have seen in previous work on $FeAl_{1-x}Cr_x$ and $FeAl_{1-x}Cu_x$. The present results show a complex magnetic behaviour of this system in contrast to that of the alloy series $FeAl_{1-x}Cu_x$ with its non-magnetic Cu as compared to magnetic Mn atoms.

Acknowledgments

I am indebted to Dr J G Booth of the University of Salford for the supply of the alloy samples. This work has been carried out at the Mössbauer Laboratory of the University of Liverpool. I wish to thank the Mössbauer group there for their assistance and the pleasant working atmosphere during my visit to their lab. I am grateful to Dr M F Thomas for the helpful discussions and comments on the manuscript. The measurements of susceptibility by S Penn is gratefully acknowledged and the assistance of Dr Q A Pankhurst and S Suharan in fitting the spectra is appreciated.

References

[1] Campbell I A 1986 *Hyperfine Interactions* **27** 15
[2] Huang C Y 1985 *J. Magn. Magn. Mater.* **51** 1
[3] Moorjani K and Coey J M D 1984 *Magnetic Glasses* (Amsterdam: Elsevier)
[4] Rainford B D and Burke S K 1982 *J. Appl. Phys.* **53** 7660
[5] Nieuwenhuys G J, Verbeek B H and Mydosh J H 1979 *J. Appl. Phys.* **30** 1685
[6] Coles B R, Sarkissian B V B and Taylor R H 1978 *Phil. Mag.* B **37** 489
[7] Boliang Yu, Coey J M D, Olivier M and Stroem-Olsen J O 1984 *J. Appl. Phys.* **55** 1748
[8] Campbell I A, Senoussi S, Varret F, Teillet J and Hmzic A 1983 *Phys. Rev. Lett.* **50** 1615
[9] Kuvano H and Ono K 1977 *J. Soc. Japan* **42** 72

[10] Niculescu V, Raj K, Budnick J I, Burch T J, Hines W and Menotti A H 1976 *Phys. Rev.* **14** 4160
[11] Shull R D, Okamoto H and Beck P A 1976 *Sol. State Commun.* **20** 863
[12] Niculescu V, Raj, K, Burch T J and Budnick J I 1976 *Phys. Rev.* **13** 3167
[13] Hines W A, Menotti A H, Budnick G I, Burch T J, Litrenta T, Niculescu V and Raj K 1976 *Phys. Rev.* B **13** 4060
[14] Murani A P 1974 *J. Phys. F: Metal Phys.* **4** 757
[15] Chacham H and da Silva E G 1986 *Phys. Rev.* B **35** 1602
[16] Saslov W M and Parker G 1986 *Phys. Rev. Lett.* **56** 1074
[17] Alcazar G A P, Plascak J A and da Silva E G 1986 *Phys. Rev.* B **34** 1940
[18] Mitra A and Ghatak S K 1985 *J. Magn. Magn. Mater.* **51** 321
[19] Jo T 1982 *J. Phys. Soc. Japan* **51** 794
[20] Gabay M and Toulouse G 1981 *Phys. Rev. Lett.* **47** 201
[21] Grest G S 1980 *Phys. Rev.* B **21** 165
[22] Shukla P and Wortis M 1980 *Phys. Rev.* B **21** 165
[23] Kirkpatrick S and Sherrington D 1978 *Phys. Rev.* B **17** 4384
[24] Johnson C E, Ridout M S and Cranshaw T E 1963 *Proc. Phys. Soc.* **81** 11079
[25] Stearns M B 1966 *Phys. Rev.* **147** 439
[26] Wertheim G K and Wernick J H 1967 *Acta. Metall.* **15** 297
[27] Okpalugo D E, Booth J G and Faunce C A 1985 *J. Phys. F: Metal Phys.* **15** 681
[28] Okpalugo D E and Booth J G 1985 *J. Phys. F: Metal Phys.* **15** 2025
[29] Saleh A S, Manikar R M, Yoon S, Okpalugo D E and Booth J G 1985 *J. Appl. Phys.* **57** 3241
[30] Kobeissi M A, Pankhurst Q A, Suharan S and Thomas M F 1990 *J. Phys.: Condens. Matter* **2** 4895
[31] Kobeissi M A, Pankhurst Q A, Penn S J and Thomas M F 1990 *J. Phys.: Condens. Matter* **2** 8639
[32] The program was achieved by Q A Pankhurst at Mössbauer Laboratory, Liverpool University, UK
[33] Le Caer G and Dubois J M 1979 *J. Phys. E: Sci. Instrum.* **12** 11083
[34] Kobeissi M A, Pankhurst Q A, Suharan S and Thomas M F 1990 *Hyperfine Interactions* **54** 817
[35] Omari I, Saleh A S and Mahmood S H 1989 *J. Magn. Magn. Mater.* **78** 183
[36] Brand R A, Lauer J and Keune W 1985 *Phys. Rev.* **31** 1630